On the induced charge density distribution in streaming plasmas

Zh.A. Moldabekov, P. Ludwig[*], J.-P. Joost and M. Bonitz

*Institut für Theoretische Physik und Astrophysik, Christian-Albrechts-Universität zu Kiel,
Leibnizstraße 15, 24098 Kiel, Germany*
[*]*e-mail: ludwig@theo-physik.uni-kiel.de*

Motivated by experiments on the generation of streaming plasmas in high energy density facilities, industrial setups, and fundamental dusty plasma research, the plasma polarization around a test charge in streaming plasmas is considered in this work. The induced charge density distribution of the plasma constituents is discussed for the subsonic, sonic, and supersonic regime taking into account the non-Maxwellian distribution of the flowing ions. It is shown that the plasma polarization (the plasma wakefield) in the vicinity of the test charge shows different scaling in the subsonic and supersonic regimes, where Mach number is defined as the ratio of the ion streaming velocity and the ion sound speed. In contrast to the wake potential, the density decays strongly monotonically in the plasma wake and does not exhibit an oscillatory pattern or trailing maxima. Therefore, the picture of an ion focusing effect creating a separated ion region downstream was not confirmed.

1. Introduction

Screening of a test charge is one of the fundamental issues of plasma physics. While screening is very well understood in the equilibrium case [1, 2], there is no consistent physical picture of this effect in streaming plasmas. Often, however, a plasma in an experiment is far from the thermodynamically equilibrium state. Therefore, the field of non-equilibrium streaming plasmas attracts broad interest. Examples of non-equilibrium plasmas with a stream of particles include complex plasmas [3, 4], dense plasmas [5, 6], so-called warm dense matter [7], and ultrarelativistic plasmas [8]. Recent experiments have been performed on the generation of streaming plasmas in high energy density facilities [9, 10, 11] as well as industrial setups [12, 13, 14]. Another very active consideration of the streaming induced phenomena such as plasma wakefields is in the field of complex plasmas, which allows for studying collective physical properties of charged many-particle systems on the kinetic level [15].

A complex (dusty) plasma is a partially ionized plasma containing additional micron or submicron sized "dust" particles that become highly charged and actively involved in various multi-component plasma processes [15]. For recent results on the dynamically screened charge potential in streaming plasmas see e.g. Refs. [4, 16, 17, 18, 19] and references therein. A main observation is that streaming leads to a significant deviation from the Yukawa-type screening. In particular, a wakefield around the test charge is formed, giving rise to an attractive force on other like-charged particles downstream. The characteristics of the wakefield potential strongly depend on the type of the energy (velocity) distribution of the plasma particles [17, 20] and on the configuration of external electric as well as magnetic fields [21].

While the potential around a test charge has been explored in detail [16, 22], an appropriate analysis of the induced charge density is still missing. To this end, in this paper, we present preliminary results of the induced charge density and analyse the relevant plasma polarization effects. The results are obtained from high resolution linear response calculations [21, 23] which have been validated against PIC simulations [20].

2. Linear response approach

In experimental complex plasmas, the non-Maxwellian distribution of the flowing ions significantly differs from shifted-Maxwellian distribution often considered in theoretical works [22, 24, 25]. Compared to a shifted-Maxwellian case, the most prominent feature of the ion wake in the non-Maxwellian case is that the screened potential has a single main maximum in the trailing wake instead of an oscillatory wakefield [18]. In contrast, the much lighter electrons can be well described by an equilibrium Maxwellian distribution.

As an ansatz, we use the dielectric function based on the non-Maxwellian distribution of the ions to calculate the induced charge density around the test charge. The dielectric function obtained in the relaxation time approximation reads [24, 26].

$$\varepsilon\left(\tilde{\mathbf{k}},0\right)=1+\frac{1}{\tilde{k}^2\tau}+\frac{1}{\tilde{k}^2+i\nu_i M\,\tilde{k}_z}\frac{1+\left\langle\xi(\mathrm{x})\,Z(\xi(\mathrm{x}))\right\rangle}{1+\left\langle\xi(0)\,Z(\xi(0))\right\rangle}\ ,\tag{1}$$

where $\left\langle...\right\rangle=\int\limits_{0}^{\infty}...\exp(-x)\mathrm{d}x$ is the average involving the following functions:

$$\xi(\mathrm{x})=\frac{\iota\nu_i-M\,\tilde{k}_z x}{\sqrt{2\left(\tilde{k}^2+\iota\nu_i M_{th}\tilde{k}_z\right)}}\ ,$$

$$Z(\mathrm{z})=\iota\sqrt{\pi}\omega(\mathrm{z})\ ,$$

$$\omega(\mathrm{z})=\mathrm{e}^{-z^2}\,\mathrm{Erfc}(-\iota\,\mathrm{z})=\frac{\iota}{\pi}\int_{-\infty}^{\infty}\frac{e^{-t^2}}{z-t}\mathrm{d}t\ .$$

In Eq. (1), $\tau=T_e/T_n$ is the electron-neutral temperature ratio, $\tilde{\mathbf{k}}$ is the wave vector in units of $\upsilon_{th}/\omega_{pi}$ (where υ_{th} is the thermal velocity of atoms and ω_{pi} is the plasma frequency of ions), and ν_i is the the ion-neutral collision frequency in units of ion plasma frequency. Additionally, the Mach number $M=\upsilon_d/c_s$ is defined as the ratio of the ion streaming velocity υ_d and the ion sound speed $c_s=\sqrt{k_B T_e/m_i}$.

In k-space, the charge density induced by a test charge Q_d can be expressed in terms of the dielectric function (1) [6]:

$$\tilde{n}_{ind}\left(\tilde{\mathbf{k}}\right)=\frac{Q_d}{e}\left(\frac{1}{\varepsilon\left(\tilde{\mathbf{k}},0\right)}-1\right)\ .\tag{2}$$

This expression is favorable for numerical evaluation. The induced charge density is then computed in real space based on a numerical three-dimensional Discrete Fourier Transformation (3D DFT) on a large grid with resolutions $4096\times4096\times16384$. In order to handle 3D grids of this size efficiently, our high performance linear response program *Kielstream* is used [27].

Without loss of generality, we consider a grain charge of $Q_d=10^4 e$. Specific parameters are the fixed temperature ratio $\tau=100$, and the ion-neutral collision frequency $\nu_i=0.01$, which is close to the collisionless case. The Mach number is varied in the range $M=0.1\ldots2.8$. We note that for very small ion streaming velocities the linear response approach may not be applicable due to strong dust-plasma interactions. Also justification of the consideration of very large values of M can be problematic due to a possible manifestation of instabilities [18, 26].

3. Results for the induced charge density distribution

As a representative example, in Figure 1, we show contour plots of the dynamically screened test charge potential and of the corresponding induced charge density distribution in the sonic case, $M=1$. In contrast to the well-known wakefield potential, where a pronounced trailing peak is present, here we find that the pattern of the induced charge density has a completely different topological structure. The induced charge density is purely monotonic. Notably, this observation contradicts the widely used picture of an ion cloud focused at some

distance from the test charge. Instead the density wake resembles a candle flame. Accordingly, this results in weaker screening at $z < 0$, and appearance of an area, at $z > 0$, where another like charged test particle is attracted [16].

The dependence of the induced charge density in the cases of subsonic and supersonic regimes are presented in Figure 2. The main feature to be noticed, is that the characteristic flame type shape is retained for all values of M. With increase of the Mach number it becomes more extended in the direction of the streaming.

In Figure 3, the induced charge density profile along z axis at $r = 0$, i.e., parallel to the streaming direction passing the test particles location, is given. Indeed, for all considered Mach numbers, there are no oscillations in the density wake field. With increase of the ion flow velocity, the induced charge density decreases in the upstream direction of the test charge, $z > 0$, while gradually increasing downstream, $z < 0$. Again, from Figure 3, one can clearly see that there are no oscillations (no maximum) in the density distribution as seen in the wake potential.
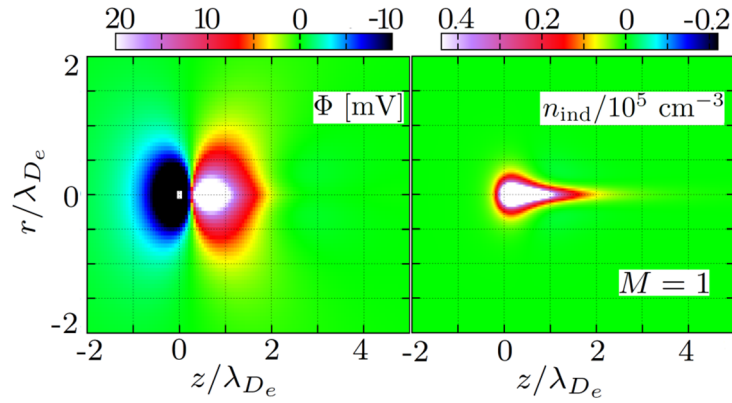

Figure 1 – Electric potential (left) and induced charge density (right) around the test charge for $M = 1$.
We use cylindrical coordinates with ions streaming in positive z-direction,
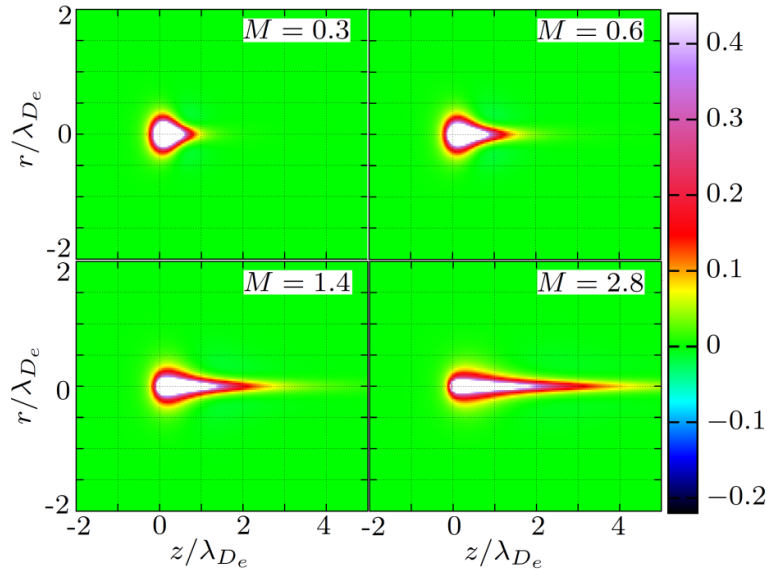where the test charge is located at the origin

Figure 2 – Induced charge density in units of 10^5 cm^{-3} for subsonic ($M = 0.3$, $M = 0.6$) and supersonic ($M = 1.4$, $M = 2.8$) regimes. For the sonic case we refer to Figure 1
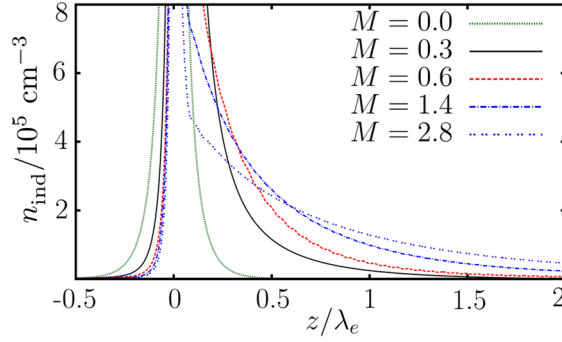
Figure 3 – Induced charge density around the test charge along streaming direction ($r = 0$)
revealing a strictly monotonic behavior

4. Characteristics of the plasma polarization

The plasma quasineutrality condition ensures that the test particle charge Q_d is compensated by the charge of the induced density distribution n_{ind} (screening cloud), i.e., $Q_{ind} = \int e\, n_{ind}\, dV = -Q_d$. This also holds in the case of streaming plasmas, where the ion streaming cannot change the charge balance.

In case of statical screening, n_{ind} is given by the Yukawa density distribution,

$$n_{ind}^Y(\mathrm{r}) = \frac{Q_d}{4\pi e} k_s^2 \frac{\exp(-\mathrm{k}_s \mathrm{r})}{r} , \qquad (3)$$

where $k_s^2 = 1/\lambda_e^2 + 1/\lambda_i^2$, and $\lambda_{e(i)} = \sqrt{k_B T_{e(i)}/4\pi e^2 n}$. In turn, in the case of dynamical screening, from the plasma quasineutrality condition, we deduce that the volume integrated deviation of n_{ind} from the Yukawa density distribution, $n_{ind}^* = n_{ind} - n_{ind}^Y$, is zero, i.e. $Q_{ind}^* = \int e\, n_{ind}\, dV = 0$. Comparison with the static case, n_{ind}^Y, yields that the charge depletion Q_{ind}^- (described by $n_{ind}^* < 0$) is equal to the charge enhancement Q_{ind}^+ (given by $n_{ind}^* > 0$). That means, the ionic Debye screening cloud around the dust particle is shifted and deformed by streaming ions but keeps its volume. The latter has been validated by direct volume integration.

In Figure 4 the value of the accommodated charge due to streaming is presented for different values of $\tau = T_e / T_n$ (100, 30, and 10). A large amount of the induced charge is displaced from the direct vicinity of the test particle downstream in the wake of the test particle. Additionally, the amount of the accommodated charge in the wakefield does not exceed the absolute value of the test particle charge. While there is a rapid increase of the accommodated charge n_{ind}^* at small M, for larger Mach numbers the wake charge slowly approaches Q_d.

So far, our consideration did not include the shape of the screening cloud (the plasma polarization) and it change during the transition from the subsonic to supersonic regime. To point this out, we consider the dipole moment due to the deformation of the induced charge density $\mathbf{d} = \int \mathbf{r}\, e n_{ind}(\mathbf{r})\, dV$. Due to symmetry of the induced charge density, $\mathbf{d}$ is directed along z axis. In Figure 5, the absolute value of $\mathbf{d}$ in units of $|Q_d|\lambda_e$ is shown as the function of the Mach number on a logarithmic scale. From this figure, one can see that the slope of dependence of $d = |\mathbf{d}|$ on M increases during the crossover from the subsonic to the supersonic regime. Therefore, the transition is well characterized by the ratio of the dipole moment to the ion flow speed, that is to say by the effective "polarizability" of the screening cloud. This quantity is presented in the inset of Figure 5. At $M < 0.5$, one finds that $d^* \sim 0.25 \times M$, and at $M > 1.5$, $d^* \sim M^2$. Therefore, the subsonic case can be characterized as linear polarization regime, whereas the supersonic case corresponds to the regime with nonlinear plasma polarization. In the subsonic regime, the linear growth of d^* with increase in the Mach number is mainly due to fast increase of the charge enhancement (see dependence of Q_{ind}^+ on M in

13

Figure 4. In the supersonic regime, where the charge enhancement changes slowly with increase in M, the dominant mechanism responsible for the quadratic growth of d^* is the displacement of the ionic screening cloud to larger distances (see Figures 2 and 3).
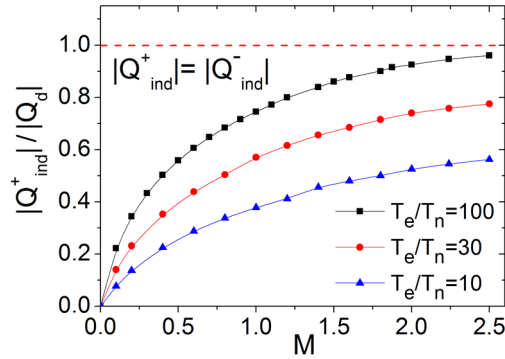

Figure 4 – Charge enhancement as function of the ion flow velocity for different electron-neutral temperature ratios
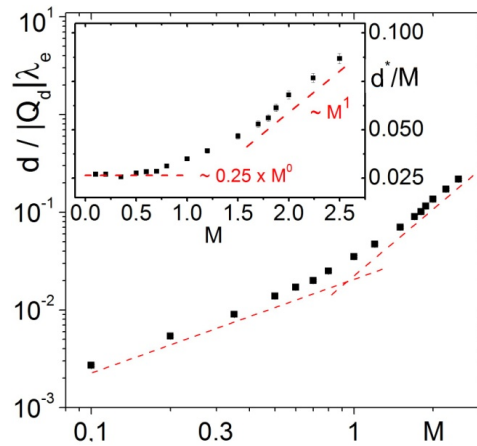

Figure 5 – Dipole moment $d^* = d / (|\,\mathrm{Q}_d\,|\,\lambda_e)$ of the induced charge density as a function of the Mach number. The transition from the linear to non-linear polarization regime is illustrated in the inset plotting the ratio of d^* to M on a linear scale. Red lines are a guide to the eye

5. Conclusions

Considering a streaming plasma, the calculation of the induced density distribution around a test charge, taking into account the non-Maxwellian distribution of the flowing ions, reveals first results for the actual plasma polarization. In particular, it has been revealed that the density profile is strictly monotonic so there are no oscillations and maximums in the wake density at all. The shape of the induced charge possesses the topology of a "candle flame". The picture of an ion focusing effect creating a separated ion region downstream is therefore questionable. At the considered parameters, the characteristic length scale of the wake density is $l \geq \lambda_e$. It remains an open question whether the field can be described at large distances $r \gg l$ using the dipole approximation.

References

1   M. Lampe, G. Joyce. Grain-grain interaction in stationary dusty plasma // Phys. Plasmas. – 2015. – Vol. 22. – P. 023704.

2   Zh. Moldabekov et al. Statically screened ion potential and Bohm potential in a quantum plasma // Phys. Plasmas. – Vol. 22. – P. 102104.

3   R. A. Quinn, J. Goree. Particle interaction measurements in a Coulomb crystal using caged-particle motion // Phys. Rev. Lett. – 2002. – Vol. 88. – P. 195001.

4   M.-J. Lee, Y.-D. Jung. Space-charge wave in a dusty plasma column containing collisional streaming ions // Physical Sciences and Technology. – 2016. – Vol. 3. – No. 2. – P. 20-24.

5   O. Hurricane et al. Fuel gain exceeding unity in an inertially confined fusion implosion // Nature. – 2014. – Vol. 506. – P. 343.

6   Zh. Moldabekov et al. Ion potential in warm dense matter: Wake effects due to streaming degenerate electrons // Phys. Rev. E. – 2015. – Vol. 91. – P. 023102.

7   N.A. Tahir et al. Proposal for the study of thermophysical properties of high-energy-density states in matter using current and future heavy ion facilities at the GSI Darmstadt // Phys. Rev. Lett. – Vol. 95. – P. 035001.

8   M.H. Thoma, Field theoretic description of ultrarelativistic electron-positron plasmas, Rev. Mod. Phys. – 2001. – Vol. 81. – P. 959.

9   F. Taccogna et al. Plasma-neutral interaction in kinetic models for the divertor region // Contrib. Plasma Phys. – 2008. – Vol. 48. – P. 147.

10   Y. Tanaka et al. Influence of emissivity on behavior of metallic dust particles in plasmas // Phys. Plasmas. – 2008. – Vol. 15. – P. 073704.

11   S. K. Kodanova et al. Dust particle evolution in the divertor plasma // IEEE Transactions on Plasma Science. – 2016. – Vol. 44. – P. 525.

12   L. Boufendi et al. Study of initial dust formation in an Ar-SiH4 discharge by laser induced particle explosive evaporation // J. Appl. Phys. – 1994. – Vol. 76. – P. 148.

13   L. Boufendi. A. Bouchoule. Industrial developments of scientific insights in dusty plasmas // Plasma Sources Science & technology. – 2002. – Vol. 11. – P. A211.

14   R.I. Golyatina, S.M. Maiorov. Ion drift in parent gas for cesium, rubidium, and mercury // Physical Sciences and Technology. – 2016. – Vol. 3. – P. 12.

15   M. Bonitz, C. Henning, D. Block. Complex plasmas – a laboratory for strong correlations // Reports on Progress in Physics. – 2010. – Vol. 73. – P. 066501.

16   P. Ludwig et al. On the wake structure in streaming complex plasmas // New J. Phys. – 2012. –Vol. 14. – P. 053016.

17   Zh. Moldabekov et al. Dynamical screening and wake effects in classical, quantum, and ultrarelativistic plasmas // Contributions to Plasma Physics. – 2015. – Vol. 55. – P. 186.

18   R. Kompaneets, G.E. Morfill, A.V. Ivlev. Wakes in complex plasmas: A self-consistent kinetic theory // Phys. Rev. E. – 2016. – Vol. 93. – P. 063201.

19   W. J. Miloch. Wake effects and mach cones behind objects // Plasma Physics and Controlled Fusion. – 2010. – Vol. 52. – P. 124004.

20   S. Sundar et al. Collision induced amplification of wakes in streaming plasmas // Phys. Plasmas. – 2017. – Vol. 24. – P. 102130.

21   J.-P. Joost et al. Screened coulomb potential in a flowing magnetized plasma // Plasma Physics and Controlled Fusion. – 2015. – Vol. 57. – P. 025004.

22   P. Ludwig et al. Non-Maxwellian and magnetic field effects in complex plasma wakes // Eur. Phys. J. D. – 2018. – Vol. 72. – P. 82.

23   P. Ludwig. C. Arran, M. Bonitz. Complex plasmas: scientific challenges and technological opportunities, edited by M. Bonitz, J. J. Lopez, K. Becker, H. Thomsen.– Springer, New York, 2014. – P. 73-99.

24   H. Kählert. Ion-dust streaming instability with non-Maxwellian ions // Phys. Plasmas. – 2015. – Vol. 22. – P. 073703.

25   K.I. Golden, G.J. Kalman, L.G. Silvestri. Is the Vlasov equation valid for Yukawa plasmas? // Physical Sciences and Technology. – 2017. – Vol. 4. – P. 9.

26   A. V. Ivlev et al. Kinetic approach for the ion drag force in a collisional plasma // Phys. Rev. E. – 2005. – Vol. 71. – P. 016405.

27   P. Ludwig, C. Arran, M. Bonitz. Introduction to streaming complex plasmas B: Theoretical description of wake effects complex plasmas: Scientific challenges and technological opportunities. – Springer, New York, 2014. – P. 73–99.